Hyperfine structure of the BaI $X\,^2\Sigma^+$ and $C\,^2\Pi$ states

W. E. Ernst[a] and J. Kändler
Institut für Molekülphysik, Freie Universität Berlin, Arnimallee 14, D-1000 Berlin 33, West Germany

C. Noda, J. S. McKillop,[b] and R. N. Zare
Department of Chemistry, Stanford University, Stanford, California 94305

(Received 16 April 1986; accepted 20 June 1986)

Optical-microwave double resonance measurements were carried out to find the hyperfine structure constants of the $v = 0$ level of the BaI $X\,^2\Sigma^+$ state. These were combined with sub-Doppler optical measurements of the BaI $C\,^2\Pi$–$X\,^2\Sigma^+$(0,0) band in order to derive the hyperfine structure constants of the excited state. We have determined the following molecular constants (in MHz) where the numbers in parentheses represent one standard deviation in a least squares fit: for the BaI $X\,^2\Sigma^+$ state, $\gamma'' = 75.8501(33)$, $b'' = 93.117(19)$, $c'' = 52.170(54)$, and $eQq'' = -33.62(12)$, and for the BaI $C\,^2\Pi$ state, $a' = 263(53)$, $b' + c' = -430(212)$, $d' = -66.7(1.4)$, and $eQq' = -214(11)$. The Fermi contact interaction and the electric quadrupole coupling constants for both the BaI X and C states appear to arise from the distortion of closed-shell I^- orbitals by the field of the Ba^+ ion. In the BaI X state, the charge distribution on the Ba^+ center is directed away from I^- while in the C state toward I^-.

I. INTRODUCTION

Barium monoiodide (BaI) is the heaviest member of the alkaline earth monohalides (MX), a family of diatomic radicals characterized by ionic bonding (M^+X^-) in which the low-lying excited states have approximately the same vibrational frequency and equilibrium internuclear distance as the ground state. Owing to its large reduced mass and to the strong preference for $\Delta v = 0$ transitions, the optical spectra of BaI are extremely congested and individual rotational lines cannot be resolved without the use of sub-Doppler techniques. Recently Johnson *et al.*[1] have reported a rotational analysis of the BaI $C\,^2\Pi$–$X\,^2\Sigma^+$(0,0) band. They accomplished this by applying the selectively detected laser induced fluorescence (SDLIF) technique[2–4] to a molecular beam of BaI. Close inspection showed that individual rotational lines were split into six hyperfine components arising from the ^{127}I nucleus with $I = 5/2$. Almost all the isotopes of Ba have no nuclear spin and hence do not contribute to these splittings.

The SDLIF method cannot be applied to low J'' transitions, and only transitions with J'' greater than 25.5 could be studied. However, the correlation between the X and C state hyperfine constants is strong for high J'' transitions. Consequently, it was not possible to deduce separately the ground and excited state hyperfine structure (hfs) constants, although ground-state excited-state differences could be determined to the accuracy of the optical experiments ($\sim$45 MHz FWHM).

In the past few years, application of optical-radio frequency[5] and optical-microwave[6] double resonance techniques to molecular beams of the alkaline earth monohalides have made it possible to observe the hyperfine structure of the ground state to an accuracy characteristic of radio frequency and microwave spectroscopy ($\leqslant$20 kHz), i.e., far superior to optical spectroscopy. Once the ground-state hyperfine structure constants have been determined, the optical data can be reanalyzed to yield the excited state hfs constants. We report here such a study on BaI in which the optical studies on the BaI $C\,^2\Pi$–$X\,^2\Sigma^+$ system were performed at the Stanford University and the optical-microwave double resonance studies on the $v'' = 0$ level of the BaI $X\,^2\Sigma^+$ state were performed at the Freie Universität, Berlin.

In what follows we describe these two experiments, show representative spectra, derive hyperfine structure constants for the BaI $X\,^2\Sigma^+$ and $C\,^2\Pi$ states, and discuss their values in terms of the bonding nature of these ionic states.

II. SPECTROSCOPIC MEASUREMENTS

A. Ground-state optical-microwave studies

Investigation of the ground-state hfs of the alkaline earth monohalides has been a topic of active interest. In reaction cells, microwave-optical polarization spectroscopy (MOPS) was successfully applied,[7] while in molecular beam experiments the highest resolution is obtained by optical-radio frequency[5] and optical-microwave[6] double resonance techniques. In a typical cell experiment, the linewidth of about 1 MHz arises primarily from the pressure and MOPS was usually applied to rotational transitions with low quantum numbers where the hfs can be well resolved. Barium monoiodide has a rotational constant of about 800 MHz[1,8] and would require investigations at 1.6 or 3.2 GHz for the study of the lowest-lying rotational transitions, not possible because of the microwave cut-off frequency of the cell apparatus in Berlin.

On the other hand, a molecular beam can be produced with reasonable BaI concentrations and in a beam experiment the linewidth for a ground-state microwave transition is only limited by the finite transit time of the molecules

[a] Present address: Department of Chemistry, Stanford University, Stanford, CA 94305.
[b] Present address: Thomas J Watson Research Center, IBM, Yorktown Heights, New York 10598.

 0021-9606/86/193735-09$02.10

through the microwave interaction region. The resulting linewidths of 10 to 50 kHz allow resolution of the hfs for microwave transitions with rotational quantum numbers up to 10, i.e., microwave frequencies up to 16 GHz. Thus the molecular beam optical-microwave double resonance technique was used for the ground-state hfs measurements.

The molecular beam apparatus for the optical-microwave double resonance spectroscopy has been described in detail in Ref. 6, and only a brief summary is provided here (see Fig. 1). A collimated beam of BaI was generated from a high temperature reaction of BaI_2 and Ba. In region A, this beam traversed a 100 mW laser beam which was tuned to a particular rotational transition in the $C\,^2\Pi$–$X\,^2\Sigma^+$ (0,0) band in order to deplete a ground state level. The population of this level was probed at B further downstream in the beam by monitoring the fluorescence induced by a second laser beam of 0.5 mW at the same wavelength. In region C between A and B, microwave radiation was introduced via a horn antenna. When microwave radiation induced a transition to the depleted level it was detected by an increase in the laser-induced fluorescence at B. Region C was well shielded from the Earth's magnetic field. Under these conditions, the linewidth was mainly determined by the time of flight of the BaI molecules through the 6 cm long microwave field. The microwave intensity was attenuated to about 5 μW/cm^2 in order to avoid saturation broadening. In this manner lines were recorded with 20 kHz FWHM.

We investigated the $N = 7 \leftarrow 6$ rotational transition in the $X\,^2\Sigma^+$ ($v = 0$) state at about 11.2 GHz. In the following, Hund's coupling case (b) notation will be employed for the description of energy levels in the electronic ground state. As shown in Fig. 2, each spin component J splits into six hfs levels due to the iodine nuclear spin $I = 5/2$. For the study of the hfs components of the rotational transition, appropriate optical lines had to be found, which pump the $J'' = 6.5$ and 7.5 levels. From the previous investigations of Johnson *et al.*[1]

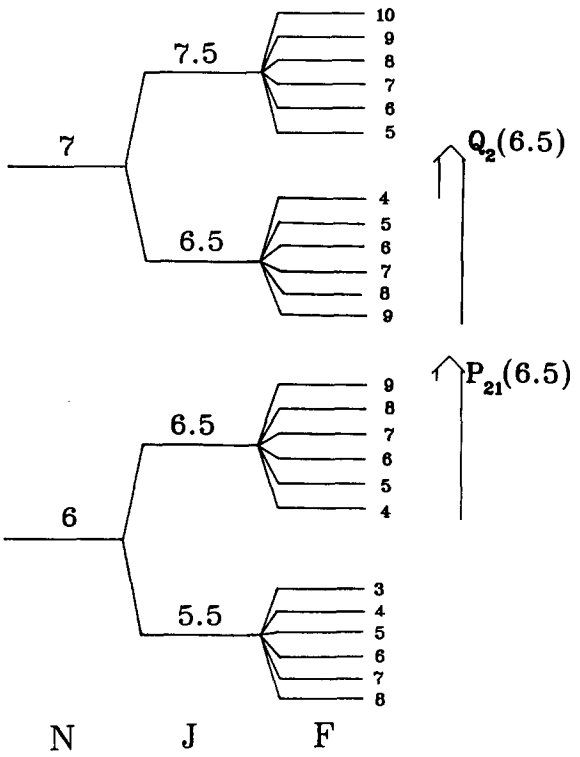

FIG. 2. Energy level diagram for the hfs components of the $N = 7 \leftarrow 6$ transition in the BaI $X\,^2\Sigma^+(v = 0)$ state. Microwave transitions with $J = 7.5 \leftarrow 6.5$ were detected when the laser was tuned to $P_{21}(6.5)$, and $J = 6.5 \leftarrow 5.5$ when the laser was tuned to $Q_2(6.5)$.

only a few lines were assigned at low J quantum numbers. After survey spectra were recorded, it was decided to choose lines in the $C\,^2\Pi_{3/2}$–$X\,^2\Sigma^+$(0,0) system near 539 nm. The wave number for the $P_{21}(7.5)$ transition was given as 18 569.113 cm^{-1} in Ref. 1. From the structure of the spectrum in this range the exact position of the $P_{21}(7.5)$ line was

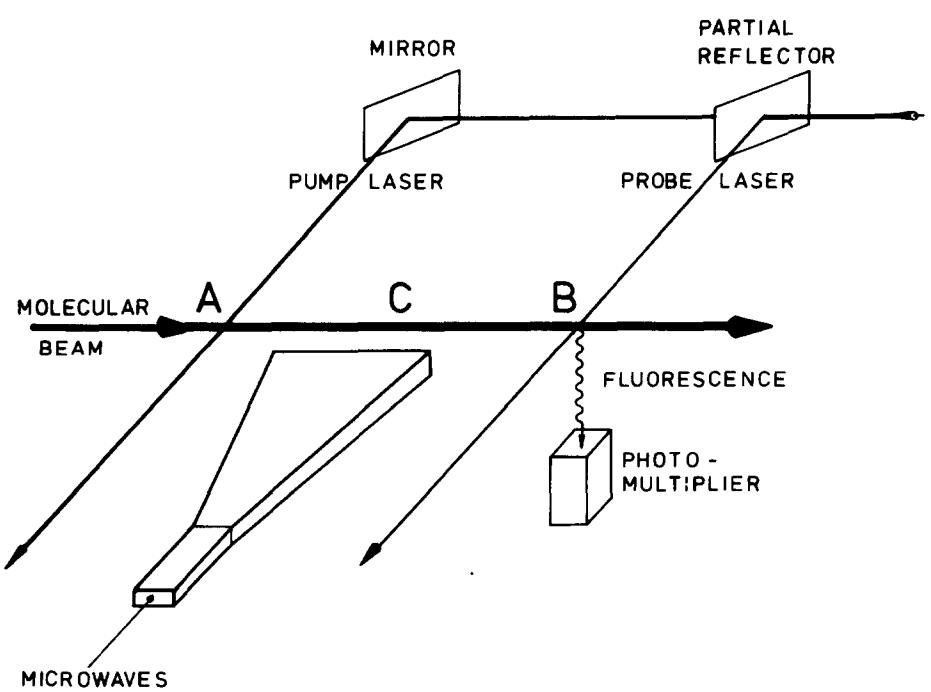

FIG. 1. Experimental apparatus used in the optical-microwave double resonance experiment.

not obvious and thus had to be identified in the double resonance experiment.

Trace (a) in Fig. 3 shows a 1.5 GHz laser scan near 18 569.14 cm^{-1}. Precise rotational constants for the $X\,^2\Sigma^+$ state were determined by Törring and Doebl[8] and a microwave frequency could be calculated for the transition $N = 7 \leftarrow 6$, $J = 7.5 \leftarrow 6.5$ without hfs. The hfs component with the highest F value, in this case $F = 10 \leftarrow 9$ (see Fig. 2), is the one which experiences the smallest shift compared to the unsplit frequency. Under the assumption that the hfs constants are of the same order of magnitude as for other alkaline earth monohalides, the line $F = 10 \leftarrow 9$ was expected to lie within a 1 MHz interval around the unsplit frequency. The procedure for finding a first double resonance signal was to tune the laser to one of the spectral peaks in the expected frequency range and to scan the microwave frequency over the predicted 1 MHz range using about 15 min of signal averaging, as described in Ref. 6.

Once a first signal was found, it became obvious that the structure around and under the line was due in part to some other optical transitions. Under these circumstances a double resonance signal suffers from the fact that repopulation of the depleted level by microwave transitions yields only a small increase in the laser-induced fluorescence signal. Thus as a next step a search was made for the $P_{21}(6.5)$ line, which was also well suited for detecting the same microwave transitions (cf. Fig. 2). The microwave frequency was fixed to the measured position for the $F = 10 \leftarrow 9$ component and the laser was slowly scanned over a range of 1.5 GHz. A second double resonance signal was recorded as shown in trace (b) of Fig. 3, and corresponded to the $F'' = 9$ component of $P_{21}(6.5)$. This line was not blended by other optical transitions and was used to detect the other five hyperfine components of the $J = 7.5 \leftarrow 6.5$ microwave transition. A typical recording of a 125 kHz microwave scan is depicted in Fig. 4. As the optical hfs had not been assigned previously for these lines, many experimental attempts were necessary to find all transitions. The final assignment is indicated in Fig. 3. With the knowledge of the ground-state rotational constants the

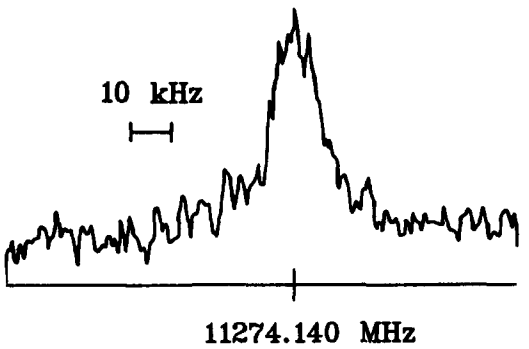

FIG. 4. A 125 kHz scan of the $F = 10 \leftarrow 9$ hyperfine component of the $N = 7 \leftarrow 6$, $J = 7.5 \leftarrow 6.5$ rotational transition. The double resonance was performed with the laser frequency fixed to the $P_{21}(6.5)$ line, and with 5 min of signal averaging.

position of the $Q_2(6.5)$ line could be estimated to lie between the $P_{21}(6.5)$ and $P_{21}(7.5)$ lines. The $Q_2(6.5)$ line was used for the detection of hfs components with $J = 6.5 \leftarrow 5.5$. The microwave transition frequencies were determined to an accuracy of about 5 kHz.

Using the optical-microwave double resonance technique described above, the microwave frequencies of ten hfs components of the $N = 7 \leftarrow 6$ rotational transition were measured; they are listed in Table I.

B. Optical studies of the BaI C–X system

The experimental apparatus is described elsewhere,[9] and a detailed explanation of the use of selectively detected laser-induced fluorescence for the detection of the BaI C–X system can be found in Ref. 10. The BaI molecule was produced in a stainless steel crucible by heating a mixture of BaI_2 and Ba at 1300 K. A 1 mm slit was placed 7 cm from the orifice to reduce the Doppler width to ~ 10 MHz.

A Coherent 599-21 dye laser was pumped by the 514.5 nm Ar^+ laser line (Coherent CR-18), and Rhodamine 560 was used with a pH = 10 buffer solution. A typical output power of 30 mW was obtained, but was reduced using neutral density filters and a dispersing telescope to avoid power

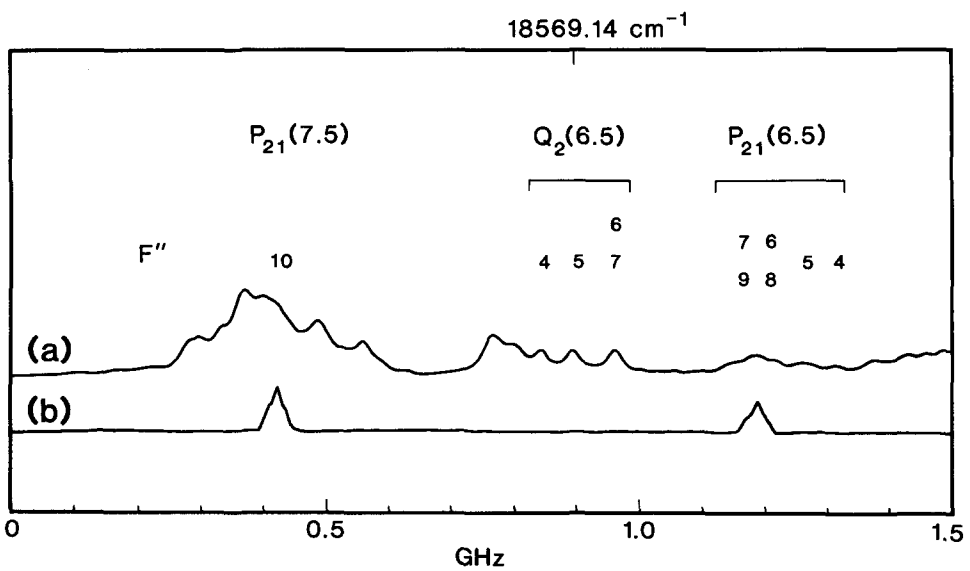

FIG. 3. A 1.5 GHz portion of the BaI $C\,^2\Pi_{3/2}$–$X\,^2\Sigma^+$ (0,0) band near 18 569.14 cm^{-1}. The energy increases to the right. Trace (a): Laser-induced fluorescence of the relevant optical lines with identification of their F'' values for the spectral features used in the double resonance experiments. The $Q_2(6.5)$ transitions are overlapped by a stronger transition. Trace (b): Laser-mw double resonance signal as the laser is scanned in the same region as in (a), while the microwave is tuned to the $N = 7 \leftarrow 6$, $J = 7.5 \leftarrow 6.5$, $F = 10 \leftarrow 9$ transition. Time constant for (a) and (b) is 3 s.

TABLE I. Measured transition frequencies of the observed hfs components of the $N = 7 \leftarrow 6$ rotational transition in the $X\,^2\Sigma^+$, $v = 0$ state of BaI. Differences between the observed and calculated values are given in the last column.

$J' - J''$	$F' - F''$	ν_{obs} (MHz)	$\nu_{obs} - \nu_{calc}$ (MHz)
6.5–5.5	4–3	11 199.429	0.003
	5–4	11 202.001	0.000
	6–5	11 202.427	0.000
	7–6	11 202.307	0.002
7.5–6.5	5–4	11 272.202	0.000
	6–5	11 271.402	0.000
	7–6	11 271.351	0.001
	8–7	11 271.798	−0.001
	9–8	11 272.716	−0.003
	10–9	11 274.140	−0.000

broadening of the transitions. The laser power at the sampling point was less than 1 mW/cm^2. The laser intersected the BaI beam at right angles, and the resulting fluorescence was monitored by a photomultiplier through a 1 m monochromator with entrance and exit slits of 150 μm. A typical count rate was 100 cps, and no signal averaging was performed.

The hyperfine structure of the BaI C–X system varies depending on the branch members observed. Figures 5–7 present representative spectra. In the $C\,^2\Pi_{1/2}$–$X\,^2\Sigma^+$ subband, the P and R branch members show well-resolved splittings while the Q branch members appear unsplit, i.e., all six hyperfine components overlap within the experimental resolution, which is the result of both residual Doppler and natural broadening. In the $C\,^2\Pi_{3/2}$–$X\,^2\Sigma^+$ subband, the hyperfine structure pattern of all rotational lines appears the same.

Twenty-eight transitions were measured in the (0,0) band of the $C\,^2\Pi$–$X\,^2\Sigma^+$ system; 18 P_{12} transitions with J'' ranging from 25.5 to 141.5, and 10 P_2 transitions with J'' ranging from 33.5 to 119.5. Most of the transitions were recorded several times. The Q branch members, whose hyperfine structure differs from the P and R branch members,

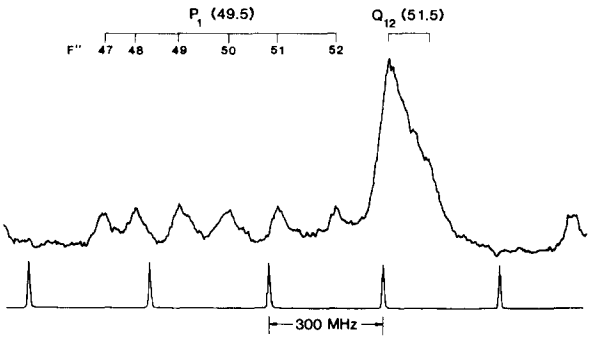

FIG. 6. Hyperfine structure of the $P_1(49.5)$ and $Q_{12}(51.5)$ transitions of the BaI $C\,^2\Pi_{1/2}$–$X\,^2\Sigma^+$ system. Frequency markers are shown on the bottom. The energy increases to the right.

were not studied, since the hyperfine components could not be resolved (see Fig. 6). Even for the lines resolved, the hyperfine components often lie too close to each other to permit an accurate measurement of their line centers. Thus, it was necessary to recover "true" line centers from the apparent line centers. This was done by assuming Lorentzian line profiles for each of the hyperfine components and calculating the peak positions from experimental peak frequencies. The line positions of all six hyperfine components could be obtained for the P_{12} transitions. On the other hand, for the P_2 transitions, two hyperfine components on the lower energy side are separated by less than their linewidth, and therefore were excluded from the analysis.

The hyperfine splittings obtained in this manner are listed in Table II. The splittings are calculated as differences between adjacent hyperfine components: For the $C\,^2\Pi_{1/2}$–$X\,^2\Sigma^+$ subband, $D_i = \nu(i) - \nu(i+1)$, $i = 1$ to 5, and $D_\Sigma = \nu(1) - \nu(6)$; and, for the $C\,^2\Pi_{3/2}$–$X\,^2\Sigma^+$ subband, $D_i = \nu(i) - \nu(i+1)$, $i = 1$ to 3, and $D_\Sigma = \nu(1) - \nu(4)$. Here $\nu(i)$ is the transition energy of the ith hyperfine component, and the "first" component is the one on the higher energy side.[11] If the transition was measured more than once, the average values are presented in Table II.

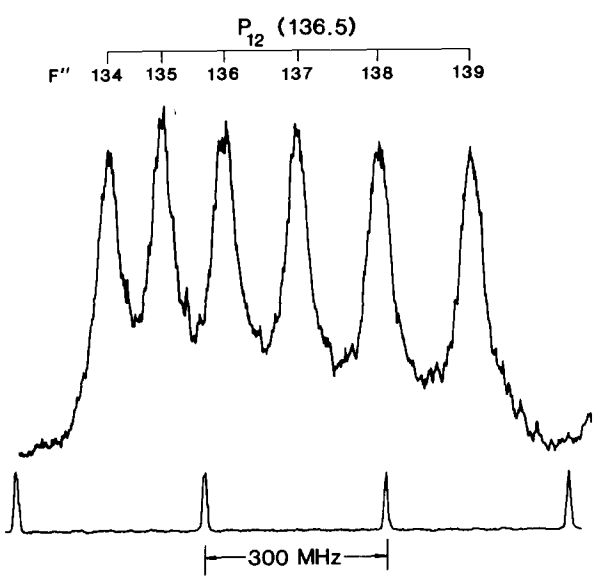

FIG. 5. Hyperfine structure of the $P_{12}(136.5)$ transition of the BaI $C\,^2\Pi_{1/2}$–$X\,^2\Sigma^+$ system. Frequency markers are shown on the bottom. The energy increases to the right.

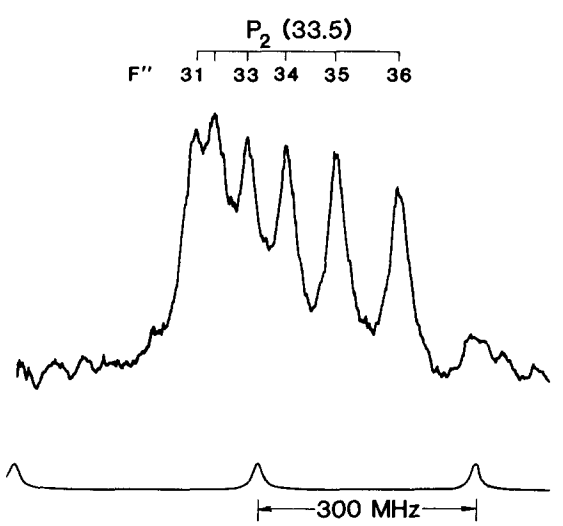

FIG. 7. Hyperfine structure of the $P_2(33.5)$ transition of the BaI $C\,^2\Pi_{3/2}$–$X\,^2\Sigma^+$ system. Frequency markers are shown on the bottom. The energy increases to the right.

TABLE II. The observed difference frequencies in MHz for the BaI $C\,^2\Pi$–$X\,^2\Sigma^+$ (0–0) band. See the text for the definition of D_i and D_Σ. The numbers in parentheses represent the difference between the observed and calculated frequencies.

Branch	J''	D_1	D_2	D_3	D_4	D_5	D_Σ
P_{12}	25.5	150 (− 2)	135 (0)	120 (1)	98 (− 7)	94 (2)	597 (− 5)
	26.5	156 (4)	133 (− 1)	121 (2)	94(− 10)	95 (3)	599 (− 2)
	28.5	149 (− 2)	133 (− 1)	117 (− 1)	107 (3)	94 (3)	599 (1)
	29.5	150 (− 0)	134 (1)	120 (2)	104 (1)	90(− 1)	599 (2)
	30.5	151 (1)	134 (1)	123 (5)	107 (4)	96 (5)	612 (16)
	38.5	149 (1)	129 (− 3)	119 (2)	105 (2)	88(− 2)	589 (0)
	39.5	147 (− 1)	129 (− 3)	118 (2)	100 (− 2)	87(− 3)	581 (− 7)
	40.5	147 (− 1)	128 (− 3)	120 (3)	96 (− 7)	87(− 2)	578 (− 9)
	41.5	150 (3)	133 (2)	119 (2)	95 (− 7)	90 (1)	587 (0)
	57.5	143 (− 3)	125 (− 6)	120 (5)	106 (5)	86(− 2)	579 (− 1)
	58.5	145 (− 0)	131 (1)	112 (− 3)	100 (− 1)	92 (4)	580 (0)
	59.5	139 (− 6)	128 (− 2)	110 (− 5)	101 (− 0)	91 (3)	569(− 11)
	60.5	141 (− 5)	129 (− 1)	113 (− 3)	103 (2)	85(− 3)	571 (− 8)
	137.5	151 (8)	136 (8)	121 (8)	104 (5)	88 (2)	600 (30)
	138.5	144 (1)	130 (2)	109 (− 4)	97 (− 2)	82(− 4)	563 (− 8)
	139.5	151 (9)	130 (2)	110 (− 4)	102 (2)	90 (4)	583 (13)
	140.5	145 (2)	129 (1)	111 (− 3)	97 (− 3)	88 (2)	570 (− 0)
	141.5	137 (− 6)	127 (− 1)	113 (− 1)	91 (− 9)	83(− 3)	550(− 20)
P_2	33.5	87 (7)	73 (8)	57 (6)	...	...	216 (21)
	34.5	71 (− 9)	56 (− 8)	47 (− 4)	...	...	174(− 20)
	35.5	76 (− 3)	62 (− 2)	49 (− 2)	...	...	187 (− 7)
	36.5	79 (− 0)	65 (0)	50 (− 1)	...	...	194 (− 0)
	54.5	70 (− 7)	56 (− 7)	45 (− 5)	...	...	171(− 19)
	55.5	89 (12)	73 (10)	57 (8)	...	...	219 (29)
	116.5	79 (3)	63 (1)	50 (2)	...	...	192 (6)
	117.5	73 (− 3)	66 (4)	47 (− 1)	...	...	186 (0)
	118.5	71 (− 5)	55 (− 6)	44 (− 4)	...	...	171(− 15)
	119.5	68 (− 8)	52(− 10)	44 (− 4)	...	...	164(− 22)

III. HYPERFINE STRUCTURE ANALYSIS AND INTERPRETATION

A. The BaI $X\,^2\Sigma^+$ state

Energies of the hfs levels of the rotational states can be calculated by diagonalization of the effective Hamiltonian

$$H = H_{\rm rot} + H_{\rm sr} + H_{\rm hfs} \tag{1}$$

with

$$H_{\rm rot} = B''\mathbf{N}^2 \tag{2}$$

and

$$H_{\rm sr} = \gamma''\mathbf{N}\cdot\mathbf{S} \tag{3}$$

describing the nuclear rotational motion and the spin-rotation interaction, respectively. The hfs Hamiltonian for the $X\,^2\Sigma^+$ state is that of Frosch and Foley[12] for the coupling case $b_{\beta J}$ with an electric quadrupole term[13]:

$$H_{\rm hfs} = b\,\mathbf{I}\cdot\mathbf{S} + cI_ZS_Z + eQq'' \times [3I_Z^2 - I(I+1)]/[4I(I-1)]. \tag{4}$$

The rotational constants were taken from the measurements of Törring and Doebl,[8] and the parameters γ'', b'', c'', and eQq'' were determined by fitting the calculated transition frequencies to the experimentally observed line positions in a nonlinear least squares procedure. The results are given in Table III and the differences between the observed and calculated frequencies are summarized in Table I.

The calculation of these parameters from first principles is presently beyond our abilities. In what follows we discuss their magnitude in terms of simple ionic bonding pictures reasoning from analogy with other alkali halides and alkaline earth monohalides. We hope in this way to gain insight into the nature of the electronic structure of BaI. We believe a fairly unified model emerges from these considerations for both the BaI *X* and *C* states.

The measured ground state fine structure and hyperfine structure constants can be compared with those of other barium monohalides. The spin-rotation interaction constants γ of the ground states of BaF,[14,15] BaCl,[14] and BaBr[16] have a size of the same order of magnitude as BaI. Usually the contribution of the second-order term $\gamma^{(2)}$ dominates the observed value of γ.[17] The mixing of rotationless electronic states induced by the rotational motion of the molecule combined with the spin-orbit interaction for the unpaired electron produces this second-order effect which can be written as

$$\gamma^{(2)} = \frac{-2\Sigma\langle n^2\Pi,v|AL_+|X\,^2\Sigma^+,v=0\rangle\langle n\,^2\Pi,v|BL_+|X\,^2\Sigma^+,v=0\rangle}{E(X\,^2\Sigma^+,v=0) - E(n\,^2\Pi,v)}. \tag{5}$$

The summation is over all $^2\Pi$ states, and A and L_+ are the spin-orbit operator and the raising operator for the orbital angular momentum, respectively. $E(X\,^2\Sigma^+,v=0)$ and $E(n\,^2\Pi,v)$ designated the energies for the $v=0$ ground state

TABLE III. Spin-rotation and hfs parameters for the $X\,^2\Sigma^+(v=0)$ and $C\,^2\Pi(v=0)$ states of BaI. The quantity in parentheses represents one standard error.

State	Parameter	Value (MHz)
$X\,^2\Sigma^+$	γ''	75.8501(33)
	b''	93.117(19)
	c''	52.170(54)
	eqQ''	−33.62(12)
$C\,^2\Pi$	a'	263(53)
	$b'+c'$	−430(212)
	d'	−66.7(1.4)
	eqQ'	−214(11)

and the nth $^2\Pi$ state in vibrational level v. The following estimate is only offered as an order of magnitude estimate of $\gamma^{(2)}$. The effect of all high-lying $^2\Pi$ states will be neglected. The first $^2\Pi$ state is $A\,^2\Pi$ at about 10 000 cm^{-1} above the ground state.[18] For all alkaline earth monohalides, the potential curves of the $X\,^2\Sigma^+$ and $A\,^2\Pi$ states are very similar and the vibrational overlap integral can be approximated by $\delta_{v'v''}$.

Then the above expression reduces to

$$\gamma^{(2)} = 2B\,\langle A\,^2\Pi, v=0|A|X\,^2\Sigma^+, v=0\rangle \times \langle A\,^2\Pi, v=0|L_+|X\,^2\Sigma^+, v=0\rangle/10\,000\ \text{cm}^{-1}. \quad (6)$$

The molecular orbital states are treated as linear combinations of atomic Ba^+ orbitals. Studies of the ground state hfs of ^{137}BaF,[14] ^{137}BaCl,[14] and ^{137}BaBr[16] yielded constants of the hfs interaction of the ^{137}Ba nucleus ($I=3/2$) with the unpaired electron. Within experimental error, the ^{137}Ba hfs constants were about the same for these monohalides. Most information about the ground state has been obtained for BaF where the fluorine hfs and the electric dipole moment have also been measured.[15] The conclusion of this work was that the ground state is represented by a combination of 76% $6s\sigma$, 21.5% $6p\sigma$, and 2.5% $5d\sigma$ centered on Ba^+. We expect that these percentages apply as well to BaI. Very little is known about the $A\,^2\Pi$ state, but we may assume a combination of 70% $6p\pi$ and 30% $5d\pi$ centered on Ba^+, as in the case of CaI.[19] The atomic Ba^+ spin-orbit constants are[20] $A(6p\ Ba^+) = 1127.24\ cm^{-1}$, and $A(5d\ Ba^+) = 320.30\ cm^{-1}$. Inserting an average B value for the $X\,^2\Sigma^+$ and the $A\,^2\Pi$ states of $2.6\times10^{-2}\ cm^{-1}$ yields $\gamma^{(2)} = 1.45\times10^{-3}\ cm^{-1}$. This should be compared to the experimental value of $2.53\times10^{-3}\ cm^{-1}$. Considering the very rough estimate, the uncertainty of the assumptions about the $A\,^2\Pi$ state, and the exclusion of higher $^2\Pi$ states, the deviation is not unreasonably large.

The value of $b(\text{I}) = 93.117(19)$ MHz and $c(\text{I}) = 52.170(54)$ MHz for the BaI $X\,^2\Sigma^+$ state are comparable to the known values for the BaF $X\,^2\Sigma^+$ and BaBr $X\,^2\Sigma^+$ states, namely, $b(\text{F}) = 63.509(32)$ MHz, $c(\text{F}) = 8.224(58)$ MHz,[15] and $b(\text{Br}) = 71(7)$ MHz.[16] The Fermi contact term $b_F'' = b'' + c''/3 = 110.54$ MHz is related to the electron spin density $|\psi(0)|^2$ at the ^{127}I nucleus by

$$b_F'' = (16\pi/3)(\mu_0\mu_I/I)|\psi(0)|^2, \quad (7)$$

where μ_0 is the Bohr magneton, μ_I the nuclear magnetic moment, and I the nuclear spin of ^{127}I. From Eq. (7), the spin density is calculated to be $|\psi(0)|^2 = 8.3513\times10^{23}\ cm^{-3}$. Measurements on the CaI $X\,^2\Sigma^+$ state by Childs *et al.*[21] yielded $b_F(\text{I}) = 159.63$ MHz. An interpretation of the Fermi contact terms of the calcium monohalides has been given by Bernath, Pinchemel, and Field.[11] They showed that the spin density on the halogen nucleus can be explained as the result of spin polarization of halogen orbitals in the field of the alkaline earth ion. The size of $b_F(\text{I})$ for the BaI $X\,^2\Sigma^+$ state indicates that the same model can be applied to the ground state of BaI.

This conclusion is supported by the small value of the electric quadrupole coupling constant eQq''. Dividing by the iodine nuclear quadrupole moment Q yields the "reduced" constant $eq'' = 42.13$ MHz, which is the product of the proton charge and the gradient of the electric field at the iodine nucleus.[22] The electric field gradient can be calculated as $q = 5.81\times10^{14}\ \text{esu cm}^{-3}$. According to Gordy and Cook,[23] the value for atomic iodine is $q_{n10} = -4.36\times10^{16}\ \text{esu cm}^{-3}$. The change of the sign and the difference by two orders of magnitude compared to the atomic value suggest that *a closed-shell negative iodine ion is distorted in the field of a positive alkaline earth ion*. As will be shown, the measured field gradient can be attributed, at least qualitatively, to this distortion by assuming the type of antishielding effect Foley, Sternheimer, and Tycko[24] proposed for other ionic molecules.

The interpretation of the observed electric quadrupole coupling constant of an alkaline earth monohalide in terms of Sternheimer antishielding has recently been discussed for the ground state of SrBr.[25] It was assumed that, for SrBr and the neighboring alkali halide RbBr, the measured coupling constants can be written as

$$eQq_{\text{meas}} = (1-\kappa)eQq_{\text{ion}}, \quad (8)$$

where q_{ion} is the gradient of the electric field of the alkali or alkaline earth ion at the halogen nucleus and κ is an effective antishielding factor. Because the same values of κ are obtained for SrBr and RbBr,[25] we examine the bonding nature of BaI by comparing it with the CsI molecule, for which $eQq_{\text{meas}} = -15.33$ MHz[26] and $r_e = 3.3151\,663(11)$ Å.[27] Using these values and assuming that the field of the alkali ion can be approximated by that of a positive point charge at a distance r_e, a field gradient can be calculated for CsI:

$$q_{\text{ion}} = \left(\frac{\partial E}{\partial r}\right)_{r_e} = \frac{2e}{r_e^3} = -2.64\times10^{13}\ \text{esu cm}^{-3}. \quad (9)$$

With $Q(^{127}\text{I}) = -7.9\times10^{-25}\ cm^2$ (Ref. 23) it follows that $eQq_{\text{ion}} = -1.51$ MHz. This implies that an antishielding factor $\kappa = -9.15$ is needed to reproduce the measured eQq value for CsI.

For BaI, Eq. (9) must be modified because of the large polarizability of the alkali earth ion, as shown in the ionic bonding model,[28] which closely reproduces the dipole moments of alkaline earth monohalides.[29] The model assumes a double positive charge at a distance r_e and a negative charge at $r_e + \Delta r$, which, respectively, represent the closed-shell metal^{2+} ion core and the single metal-centered electron

whose center of charge is shifted by Δr away from the halogen (cf. Fig. 1 of Ref. 28). Then the field gradient at the halogen nucleus is given as[25]

$$q_{\text{ion}} = \left(\frac{\partial E}{\partial r}\right)_{r_e} = -\frac{4e}{r_e^3} + \frac{2e}{(r_e+\Delta r)^3}\left(1+\frac{\partial \Delta r}{\partial r}\right), \quad (10)$$

where the first term represents the contribution by the metal^{2+} ion and the second term by the electron. Inserting r_e(BaI) = 3.084 798(11) Å[8] and Δr = 1.0 Å,[28] we obtain $q_{\text{ion}} = -6.34\times10^{13}$ esu cm^{-3} and $eQq_{\text{ion}} = -3.63$ MHz. Consequently a value of $\kappa = -8.17$ is required to reproduce $eQq_{\text{meas}} = -33.63$ MHz, and the antishielding factor for BaI is very close to that of CsI. This indicates that *for the BaI $X\,^2\Sigma^+$ state the field gradient at the iodine nucleus is dominated by the metal^{2+} core* due to the strong r^{-3} dependence, as opposed to the alkali$^+$ core in CsI.[25] The effective antishielding factor differs significantly from the calculated Sternheimer antishielding parameter γ_∞,[24] which ranges from -138 to -175 for I^- depending on the approach used in the calculation.[30]

Unfortunately, the theoretically derived antishielding factors of the halogens always turned out to be very large and the measured coupling constants of the alkali halides could explain only antishielding effects smaller by an order of magnitude. This has generally been explained by the fact that halogen ions are particularly easily distorted. Thus many other effects could be responsible for partially canceling the antishielding distortion. The above estimate is primarily intended to show that the difference of a factor of 2 in the size of eQq values of the alkaline earth monohalides and the corresponding alkali halides can be explained by the different charge distribution at the metal nucleus, as pointed out in Ref. 25.

In summary, ionic bonding in which the positive alkaline earth ion distorts the charge distribution on the negative halogen ion can explain both the magnetic and electric quadrupole hyperfine structure of the BaI ground state.

B. The BaI $C\,^2\Pi$ state

The model used here is based on the Frosch and Foley Hamiltonian[12] with an additional term representing the electric quadrupole interaction[13]

$$H_{\text{hfs}} = a'\Lambda\mathbf{I}\cdot\mathbf{K} + b'\mathbf{I}\cdot\mathbf{S} + c'(\mathbf{I}\cdot\mathbf{k})(\mathbf{S}\cdot\mathbf{k}) + eQq'[3I_z^2 - I(I+1)]/[4I(I-1)]. \quad (11)$$

Case a_β-type coupling[22] is assumed for the $C\,^2\Pi$ state. Then the hyperfine energy levels can be written as

$$E(J,\Omega,\Sigma,F) = [a' + (b'+c')\Sigma]\Omega C/2J(J+1) - eQq'Y(F,I,J)[1 - 3\Omega^2/J(J+1)], \quad (12)$$

where

$$C = F(F+1) - I(I+1) - J(J+1), \quad (13)$$

and $Y(F,I,J)$ is Casimir's function

$$Y(F,I,J) = \frac{(3/4)C(C+1) - I(I+1)J(J+1)}{2I(2I-1)(2J-1)(2J+3)}. \quad (14)$$

It should be noted that the b' and c' constants are not separable in this case, and only the sum of the two can be determined. In addition, for the $^2\Pi_{1/2}$ state, there is an e/f parity-dependent term

$$\pm dC(F,I,J)/[4J(J+1)], \quad (15)$$

where the plus sign refers to e-parity states, and the minus sign to f-parity states.

The hfs constants have the traditional interpretation that[12,22]

$$a' = \frac{2\mu_0\mu_I}{I}\left(\frac{1}{r^3}\right)_{\text{ave}}, \quad (16)$$

$$b' = \frac{3\mu_0\mu_I}{I}\left(\frac{16\pi}{3}|\psi(0)|^2 - \left[\frac{3\cos^2\theta - 1}{r^3}\right]_{\text{ave}}\right), \quad (17)$$

$$c' = \frac{3\mu_0\mu_I}{I}\left(\frac{3\cos^2\theta - 1}{r^3}\right)_{\text{ave}}, \quad (18)$$

$$d' = \frac{3\mu_0\mu_I}{I}\left(\frac{\sin^2\theta}{r^3}\right)_{\text{ave}}, \quad (19)$$

and

$$eQq' = eQ\left(\frac{3\cos^2\theta - 1}{r^3}\right)_{\text{ave}}. \quad (20)$$

In these expressions, r is the distance between the electron and the magnetically active nucleus and θ the angle between r and the internuclear axis. In Eq. (16), the average is taken over *the electrons which provide orbital angular momentum* whereas in Eqs. (17)–(19) averages are taken over *the electrons which provide spin-angular momentum*. In the case of the quadrupole coupling constant eQq' [Eq. (20)], the expression has to be averaged over *all electrons in the molecule*.

A least squares fit was used to determine the excited state hyperfine parameters, while the ground-state parameters, obtained from the optical-microwave double resonance studies, were held fixed. The results are shown in Table III, and the differences between the observed and calculated splittings are listed in Table II. The standard deviation of the fit was 8.2 MHz.

At first sight, this set of excited state hfs parameters looks very puzzling. Very often spin and orbital angular momenta are provided by the same electrons and the relation

$$c' = 3(a' - d') \quad (21)$$

can be derived from Eqs. (16), (18), and (19). Inserting the values of a' and d' from Table III yields c' = 889 MHz. The quadrupole coupling constant can be separated into two contributions as

$$eQq' = (eQq)_{\text{el}} + (eQq)_{\text{pol}}. \quad (22)$$

The first term is due to the electrons responsible for the anisotropic magnetic coupling constant c' and therefore given by

$$(eQq)_{\rm el} = -\frac{Ie^2Qc'}{3\mu_0\mu_{\rm I}} = 1.16c'$$
$$= 1032 \text{ MHz} \qquad (23)$$

for $c' = 889$ MHz and $Q(^{127}\text{I}) = -7.9\times10^{-25}$ cm^2 (Ref. 23). In order to obtain the measured quadrupole coupling constant, the term $(eQq)_{\rm pol}$, which is due to polarization of closed shells, would have to be unreasonably large (about -1200 MHz). Thus we conclude that Eq. (21) does not hold, i.e., *the spin and orbital angular momenta responsible for the hfs interaction in the BaI C state involve different electrons.*

Another indirect conclusion can be drawn concerning the Fermi contact term $b'_F = b' + c'/3$, which gives the electron spin density at the iodine nucleus [cf. Eq. (8)]. In what follows we argue that this value is probably negative. In order to obtain a positive spin density, $b' + c'/3$ must be positive, and this requires that c' must be less than -645 MHz, since $b' + c' = -430$ MHz according to the measurements. The electric quadrupole coupling constant for an atomic p electron of iodine is $eQq_{n10} = 2292.44$ MHz[23] and the eQq parameter for the BaI C state indicates nearly closed iodine p shells. This means that the electron responsible for c' must not be in the iodine closed shell, and cannot interact with the iodine nucleus to give $c' \leqslant -645$ MHz. Therefore, we conclude that *the value of c' is small in absolute magnitude and the Fermi contact term and the spin density at the iodine nucleus must be negative.*

This conclusion casts some light on the bonding picture of the $C\,^2\Pi$ state. In larger molecules, a negative Fermi contact interaction is more commonly observed and is explained as follows.[31] An unpaired electron in a π orbital localized outside the core around the iodine nucleus experiences different exchange interaction with the two σ electrons in closed s shells of the iodine core. Spin polarization arises due to the preferred exchange interaction of the π electron with the σ electron whose spin is parallel. The **I·S** term in the hfs Hamiltonian is larger for the σ electron with antiparallel spin than for the one interacting more strongly with the π electron. Therefore the difference

$$|\psi_{ns\uparrow}(0)|^2 - |\psi_{ns\downarrow}(0)|^2 \qquad (24)$$

is negative if the π electron has spin up ($\uparrow$). This spin polarization effect requires a single π electron located between the Ba^{2+} and I^- cores in order to obtain the value of b'_F observed here. In fact this picture is rather appealing for the $C\,^2\Pi$ state. In the excited states of CaCl, Klynning and Martin[32] suggested a mixing of $4p\pi$ and $3d\pi$ states and assumed orthogonality of the A and C state wave functions. Consequently the orbitals would be strongly polarized, away from Cl^- for $A\,^2\Pi$ and toward Cl^- for $C\,^2\Pi$. In another study of the calcium monohalides Rice, Martin, and Field[33] suggest the mixing of higher $np\pi$ orbitals but because of the considerable $4p\pi$ and $3d\pi$ contributions they also conclude that the electron should be polarized toward the halogen in the $C\,^2\Pi$ state. This means that *for the BaI $C\,^2\Pi$ state the single unpaired Ba electron is in a molecular orbital made up from $6p\pi$, $5d\pi$, $7p\pi$ and higher Ba^+ orbitals with the center of charge shifted toward I^-*, and that *spin polarization of closed I^- s shells due to this electron causes the negative Fermi contact term.* In this picture for the $C\,^2\Pi$ state, the s shells on $^{127}I^-$ are distorted slightly toward Ba^+, and two lobes of the p–d hybrid π orbital partially reach the closed iodine shells increasing the value of $(1/r^3)_{\rm ave}$ for the single π electron. This can explain the magnitude of the hyperfine parameter a'. From the above arguments, it becomes clear that the interaction of different electrons with the iodine nucleus is responsible for the magnetic hfs constants a', $b' + c'/3$, and d' causing the usual relation between a', b', and c' to fail.

With this bonding picture, it is difficult to determine the bonding character in percentages of covalency or ionicity. The usual comparison of molecular and atomic quadrupole coupling constants is based on the theory of Townes and Dailey.[34] The measured quadrupole coupling constant is related to the atomic parameter by

$$eQq_{\rm meas} = -\frac{(1-i_c)(1-a_s^2)}{1+i_c\epsilon}\,eQq_{n10}\,, \qquad (25)$$

where i_c is the ionicity of the bond, a_s^2 a mixing coefficient for s hybridization of the bonding orbital, and ϵ a factor applied to correct for the change in nuclear screening caused by the negative charge of the size i_c. The spin polarization effect discussed for the Fermi contact interaction suggests that the application of Eq. (25) to the BaI $C\,^2\Pi$ state may be difficult. Neglecting any hybridization, an ionicity $i_c = 89\%$ can be derived. On the other hand, Eq. (25) cannot answer the question which electrons spend part of the time in a bonding orbital. Mixing coefficients of this orbital are unknown and therefore the estimate of i_c has to remain doubtful. The model calculation of Rice, Martin, and Field[33] assumes 100% ionicity for the X, A, B, and C states of the calcium monohalides. However, they conclude that the $C\,^2\Pi$ state is less well represented by the ligand field model and will be more susceptible to covalent effects. Under the assumption of 100% ionicity, the measured electric quadrupole coupling constant of the BaI $C\,^2\Pi$ state would have to be due only to polarization effects. In the ground state, these polarization effects could be accounted for by using the idea of Sternheimer antishielding. This discussion, however, cannot be applied to the C state, because the suggested charge distribution does not allow a simple calculation based on the use of point charges. In other words, the metal-based charges causing the electric field gradients are too close to the iodine orbitals for using any fixed antishielding factors, if 100% 100% ionicity is assumed.

Another consistency check can be made to test whether the polarization of closed shells can be responsible for $eQq'_{\rm meas}$. If the quadrupole coupling constant and the magnetic hfs constant c' are both caused by the same I^- electrons, i.e., those responsible for the negative Fermi contact interaction, eQq' and c' should obey the relation

$$c' = -\frac{3\mu_0\mu_{\rm I}}{Ie^2Q}\,eQq'_{\rm meas}$$
$$= -184.5 \text{ MHz}. \qquad (26)$$

Using the values of $b' + c'$ given in Table III, it follows that $b' = -245.5$ MHz and $b_{F'} = b' + c'/3 = -307$ MHz, a reasonable value when compared with the value for the ground state $b''_F = 110.54$ MHz. Spin polarization can be

used to interpret these Fermi contact interaction parameters successfully: *A σ-type Ba^+ orbital polarized away from I^- is responsible for the magnitude and sign of the hfs parameters in the ground state, while a π-type Ba^+ orbital polarized toward I^- is responsible for the one in the excited state.* Further experiments, such as the measurement of the excited state electric dipole moment, could test this picture for the bonding nature of the BaI *C* state.

ACKNOWLEDGMENTS

The authors wish to thank Professor T. Törring for many stimulating discussions, and Professor R. W. Field and Professor P. F. Bernath for comments on the manuscript. The Berlin part of the work was financially supported by the Deutsche Forschungsgemeinschaft in the Sfb 161. The Stanford part of the work was supported by The U. S. National Science Foundation under NSF CHE 85-05926. WEE is a Heisenberg fellow. CN is grateful to Janet R. Waldeck for her comments and discussions.

[1]M. A. Johnson, C. Noda, J. S. McKillop, and R. N. Zare, Can. J. Phys. **62**, 1467 (1984).
[2]W. Demtröder, in *Case Studied in Atomic Physics*, edited by M. R. C. McDowell and E. W. McDaniels (North-Holland, Amsterdam, 1976), Vol. 6.
[3]C. Linton, J. Mol. Spectrosc. **69**, 351 (1978).
[4]M. Dulick, P. F. Bernath, and R. W. Field, Can. J. Phys. **58**, 703 (1980).
[5]W. J. Childs and L. S. Goodman, Phys. Rev. A **21**, 1216 (1980).
[6]W. E. Ernst and S. Kindt, Appl. Phys. B **31**, 79 (1983).
[7]W. E. Ernst and T. Törring, Phys. Rev. A **27**, 875 (1983).
[8]T. Törring and K. Doebl, Chem. Phys. Lett. **115**, 328 (1985).
[9]C. T. Rettner, L. Wöste, and R. N. Zare, Chem. Phys. **58**, 371 (1981).
[10]C. Noda, J. S. McKillop, M. A. Johnson, J. R. Waldeck, and R. N. Zare, J. Chem. Phys. **85**, 856 (1986).
[11]P. F. Bernath, B. Pinchemel, and R. W. Field, J. Chem. Phys. **74**, 5508 (1981).
[12]R. A. Frosch and H. M. Foley, Phys. Rev. **88**, 1337 (1952).
[13]H. E. Radford, Phys. Rev. A **136**, 1571 (1964).
[14]C. Ryzlewicz, H.-U. Schütze-Pahlmann, J. Hoeft, and T. Törring, Chem. Phys. **71**, 389 (1982).
[15]W. E. Ernst, J. Kändler, and T. Törring, J. Chem. Phys. **84**, 4769 (1986).
[16]W. E. Ernst, G. Weiler, and T. Törring, Chem. Phys. Lett. **121**, 495 (1985).
[17]R. N. Zare, A. L. Schmeltekopf, W. J. Harrop, and D. L. Albritton, J. Mol. Spectrosc. **46**, 37 (1973).
[18]K. P. Huber and G. Herzberg, *Molecular Spectra and Molecular Structure. IV. Constants of Diatomic Molecules* (Van Nostrand Reinhold, New York, 1979).
[19]D. E. Reisner, P. F. Bernath, and R. W. Field, J. Mol. Spectrosc. **89**, 107 (1981).
[20]C. E. Moore, *Atomic Energy Levels I-III* (National Bureau of Standards, Washington, D.C., 1949–1958).
[21]W. J. Childs, G. L. Goodman, L. S. Goodman, and V. Pfeufer, J. Mol. Spectrosc. **107**, 94 (1984).
[22]C. H. Townes and A. L. Schawlow, *Microwave Spectroscopy* (Dover, New York, 1975).
[23]W. Gordy and R. L. Cook, *Microwave Spectra* (Wiley, New York, 1984).
[24]H. M. Foley, R. M. Sternheimer, and D. Tycko, Phys. Rev. **93**, 734 (1954).
[25]W. E. Ernst and J. O. Schröder, Z. Phys. D **1**, 103 (1986).
[26]R. Tischer (private communication). Also see *Landolt-Börnstein, New Series II/6* (Springer, Berlin, 1974); *New Series II/14a* (Springer, Berlin, 1982).
[27]J. Hoeft, E. Tieman, and T. Törring, Z. Naturforsch. Teil A **27**, 1017 (1972).
[28]T. Törring, W. E. Ernst, and S. Kindt, J. Chem. Phys. **81**, 4614 (1984).
[29]W. E. Ernst, J. Kändler, and T. Törring, Chem. Phys. Lett. **123**, 243 (1986).
[30]E. A. C. Lucken, *Nuclear Quadrupole Coupling Constants* (Academic, London, 1969).
[31]D. A. Goodings, Phys. Rev. **123**, 1706 (1961); A. Carrington and A. McLachlan, *Introduction to Magnetic Resonance* (Harper and Row, New York, 1967), especially pp. 81–83.
[32]L. Klynning and H. Martin, Phys. Scr. **24**, 33 (1981).
[33]S. F. Rice, H. Martin, and R. W. Field, J. Chem. Phys. **82**, 5023 (1985).
[34]C. H. Townes and B. P. Dailey, J. Chem. Phys. **17**, 782 (1949); Phys. Rev. A **74**, 1245 (1949).